Available online at www.sciencedirect.com
SCIENCE DIRECT®
Journal of Pharmaceutical and Biomedical Analysis
34 (2004) 945–956
JOURNAL OF PHARMACEUTICAL AND BIOMEDICAL ANALYSIS
www.elsevier.com/locate/jpba

Penciclovir solubility in Eudragit films: a comparison of X-ray, thermal, microscopic and release rate techniques

A. Ahmed [a], B.W. Barry [a], A.C. Williams [a,*], A.F. Davis [b]

[a] *Drug Delivery Group, School of Pharmacy, University of Bradford, Bradford, West Yorkshire BD7 1DP, UK*
[b] *GlaxoSmithKline Consumer Healthcare Brands, Weybridge, Surrey, UK*

Received 27 July 2003; received in revised form 17 November 2003; accepted 21 November 2003

Abstract

The solubility of penciclovir ($C_{10}N_5O_3H_{17}$) in a novel film formulation designed for the treatment of cold sores was determined using X-ray, thermal, microscopic and release rate techniques. Solubilities of 0.15–0.23, 0.44, 0.53 and 0.42% (w/w) resulted for each procedure. Linear calibration lines were achieved for experimentally and theoretically determined differential scanning calorimetry (DSC) and X-ray powder diffractometry (XRPD) data. Intra- and inter-batch data precision values were determined; intra values were more precise. Microscopy was additionally useful for examining crystal shape, size distribution and homogeneity of drug distribution within the film. Whereas DSC also determined melting point, XRPD identified polymorphs and release data provided relevant kinetics.

Keywords: Eudragit films; Drug solubility; X-ray powder diffraction; Differential scanning calorimetry; Light microscopy; Release kinetics; Penciclovir

1. Introduction

Penciclovir [9-(4-hydroxy-3-hydroxymethylbut-1-yl)guanine], a synthetic nucleoside analogue, is a potent inhibitor of *Herpes simplex virus* (HSV1 and 2). It has been marketed in topical preparations (Vectavir/Denavir) for the treatment of cold sores. A semi-solid polymer formulation of penciclovir ($C_{10}N_5O_3H_{17}$) has been developed, which upon application to the affected area, rapidly dries leaving a thin protective film. This layer is clear, dry to touch, substantive and aesthetically acceptable.

It is important to characterise drug solubility within such a transdermal drug delivery system to understand and predict in vivo performance of the product [1]. The thermodynamic activity of the drug in the vehicle describes the potential of the active ingredient to become available for its therapeutic purpose, i.e. the leaving potential. Higuchi [2] postulated that to achieve the maximum rate of drug penetration, the highest thermodynamic potential should be utilised; this is usually a saturated system. The level of saturation depends on the amount and solubility of the drug in the vehicle and other factors such as the addition of solubility enhancers (e.g. propylene glycol), which may result in

* Corresponding author. Tel.: +44-1274-234756; fax: +44-1274-234769.
E-mail address: a.c.williams@bradford.ac.uk (A.C. Williams).

0731-7085/$ – see front matter © 2003 Elsevier B.V. All rights reserved.
doi:10.1016/j.jpba.2003.11.018

a sub-saturated system and hence reduce the rate of drug delivery. Many formulations overcome problems caused through using solubility enhancers by adding excessive amounts of drug to the formulation, leading to wastage of the active ingredient and poor efficiency of the product. Increasing the drug loading within a preparation does decrease potential problems caused by depletion of the active ingredient. Contrary wise, a high solubility may reduce drug partitioning into the skin. Therefore, bases selected should balance optimum solubility and release properties [1]. Also, knowledge of the physical state of the drug (dissolved or suspended) in the vehicle is required to model appropriately its release kinetics [3].

Hence, the solubility of a drug in its medium is an important determinant in formulation efficacy. However, it is difficult to measure such solubilities in semi-solids and films. Conventional methods such as filtration of a saturated drug solution and analysis [4] are inappropriate as it is difficult to remove excess crystals.

Several techniques have been used in attempts to measure solubility in semi-solids and films. For oxybenzone, Kobayashi and Saitoh [5] collected the residual liquid separated from an ointment on storage and measured concentration. They confirmed the absence of crystals by microscopy, and the solubility determined by the residual liquid approach was in a range consistent with microscopic examination. Optical methods for solubility measurements have also provided accurate data. Gopferich and Lee [6] measured clenbuterol solubility in polymer films; visible microscopy was the most sensitive of their techniques, with detection limit of 10% (w/w) compared to differential scanning calorimetry (DSC) and release studies (limits were 12 and 13.5% (w/w), respectively).

DSC has also been utilised to determine solubility of cholesterol in a silicone matrix [7] and for measuring propranolol [8], salicylic acid and chlorpheniramine [9] dispersed in polymer films. Plots of drug concentration versus enthalpy of fusion and extrapolation to the intersect provided data for the drugs, although clearly these determinations provided solubilities at the melting point, not at room (or skin) temperature.

Infra red attenuated total reflectance (IR-ATR) spectroscopy can determine solubility in acrylate adhesives [10,11]. The colorimetric determination of betamethasone in a topical vehicle by oxidation and then condensation of the 17 α-ketol group with phenylhydrazine has also been successfully demonstrated [12]. Chowhan and Pritchard [13] used partition data between the vehicle and an aqueous phase, together with release data, to determine concentrations of corticoids in ointment bases.

Interestingly, salicylic acid solubility in a hydrogel has been determined by X-ray powder diffractometry (XRPD). The intensities of salicylic acid peaks from its XRPD trace were linearly related to its weight percent in the formulation. The solubility of the acid in the hydrogel was taken as the intercept, determined to be 20% (w/w), but there was a large variance associated with this measure [14].

The objective of our work was to investigate the suitability of microscopy, DSC, XRPD and release experiments for determining penciclovir solubility in Eudragit NE30D films. Linear calibration lines were constructed for the DSC and XRPD data, intra- and inter-batch reproducibility of data was also determined. The solubility values from each of the methods were compared and advantages and disadvantages of the techniques were considered.

2. Experimental

2.1. Materials

Penciclovir (>99%, GSK, Weybridge, UK) was used as obtained, Eudragit NE30D (poly(ethyl acrylate methyl methacrylate)) was sourced from Rhom Pharma (Darmstad, Germany) and thickener Plasadone K90 (poly(vinylpyrolidine) (PVP)) was from ISP (Wayne, USA). HPLC grade methanol, buffer salt potassium dihydrogen orthophosphate and lithium fluoride standard (>99%) were supplied by Sigma (Dorset, UK).

2.2. Formulation preparation

The thickener PVP (0.5 g) was well stirred into the Eudragit NE30 dispersion (9.5 g). Penciclovir, 0.025–10% (w/w) were mixed into the vehicle and equilibrated overnight; three batches for each drug loading were prepared. A film forming aid or plasticizer was not required since soft flexible films resulted after drying at 32 °C.

2.3. Film casting

Films for microscopy, DSC and XRPD analysis were cast within a PVC template on a Teflon coated glass to obtain uniform sheets. The deposits were dried at 32 °C for 24 h; thickness of dry films was 0.5 ± 0.1 mm ($n = 30$). Films were stored in a humidity cabinet at 32 °C at 38% r.h.

2.4. Penciclovir loading in cast films

Penciclovir content in the films were assessed by dissolving 100 mg samples in 10 ml ethanol before HPLC determination. Three samples at each drug concentration from all three batches ($n = 9$), assessed drug homogeneity.

2.5. HPLC analysis

Penciclovir was analysed using a Hewlett-Packard 1100 HPLC instrument, with a flow rate of 1 ml min^{-1}, column temperature 30 °C, UV detection at λ_{max} of 254 nm and an injection volume of 100 μl. The mobile phase was composed of methanol–potassium phosphate (pH 7.0; 23 mM; 10:90 (v/v)), filtered and degassed. A guard column (Hypersil ODS C_{18} RP, 5 μm, 2.1 mm × 20 mm) cleaned the injected sample prior to separation on the main column (Hypersil ODS C_{18} 5 μm, 150 mm). The method gave a linear response with concentration over the range 0–100 μg ml^{-1} with $r^2 = 0.9999$; limit of detection was 0.016 μg ml^{-1} and limit of quantification 0.055 μg ml^{-1}.

2.6. Microscopy

Films were examined under a visible microscope (Nixon labophot 2A) at 20× magnification for the presence of penciclovir crystals and photographs taken with a Nikon C35 camera (Nikon, Japan).

2.7. Differential scanning calorimetry (DSC)

Temperature and enthalpy were calibrated with an indium standard and the thermal behaviour of the films was examined using DSC (Perkin-Elmer Series 7) using 10 °C min^{-1} over 25–300 °C. Samples in triplicate (8–10 mg), sealed in aluminium pans, were scanned against an empty reference pan. Since penciclovir content ranged from 10 to 0.025% (w/w), sample weights were so as to maintain constant drug amounts.

The enthalpy of fusion of penciclovir was calculated from the melting endotherm using Perkin-Elmer Pyris Software. The solubility at its melting point was determined from the intercept of a plot of enthalpy of fusion (J g^{-1}) versus drug loading (% (w/w)).

2.8. X-ray powder diffractometry (XRPD)

A Siemens D5000 powder diffractometer (Siemens, Karlsruhe, Germany) equipped with a scintillation counter detector produced film diffractograms. After calibration with lithium fluoride, samples were exposed to Cu Kα radiation, wavelength 1.5418 Å, through 2 nm slits from 2 to 60° 2θ with a step size of 0.05° 2θ and a count time of 1 s per step; the generator was set to 40 kV and 30 mA.

Samples (area = 3 cm^2) were weighed and placed in holders with triplicate determination of Batch 1 and one analysis for Batches 2 and 3, allowing calculation of intra- and inter-batch variation.

Integrated peak intensities (peak areas) were calculated from the diffractograms using GRAMS 32 version 5 software (Galactic Industries Corporation, USA). Integrated data were produced for five peaks in each diffractogram ($2\theta = 8, 11, 17, 18, 26°$), summed and adjusted for sample weight. A plot of I/I_0 (I: sum of five peaks at particular weight fraction, I_0: sum of five peaks for pure penciclovir powder) versus the weight fraction of drug yielded an intercept that provided the solubility.

2.9. Penciclovir release studies

Films were cast into holders (area = 1 cm^2) and placed in a oven for 24 h at 32 °C. A modified USP XXI rotating paddle method [8] determined the release. The receptor was 250 ml of a 10 mM pH 7.4 phosphate buffer maintained at 32 ± 1 °C (representing surface skin temperature) agitated by paddles at 50 rpm ensured sink conditions. Aliquots were removed at intervals, analysed using HPLC and replaced by fresh media. Formulations were tested in triplicate and release data were plotted according to Eq. (10). Solubility was determined from the differences in the rate of increase in the release rate constant as a function of drug loading.

2.10. Precision of data

Precision was assessed using percentage relative standard deviation (%R.S.D.) calculated as:

$$\%\text{R.S.D.} = \frac{\text{S.D.}}{\text{mean}} \times 100 \quad (1)$$

The precision for each point on the calibration plots was calculated for intra- and inter-batch data ($n = 3$).

3. Results and discussion

3.1. Penciclovir concentration in films

Casting the semi-solid formulations and solvent loss upon drying concentrated the drug in the resulting films. The concentration of penciclovir was determined using an HPLC assay (see Table 1). Data precision was within 4% R.S.D. indicating that the drug was homogeneously distributed for the 100 mg sample size tested.

3.2. Microscopy

Microscopic examination provided direct visual evidence for the presence or absence of solid penciclovir in the films with needle shaped crystals evident at high concentrations (Fig. 1A). As the penciclovir loading decreased, the number of crystals declined until at 0.23% (w/w) only a few fragments were visible; at 0.15% (w/w) none were apparent (Fig. 1B). Based on these observations, penciclovir solubility was estimated to be between 0.23 and 0.15% (w/w). The absence of any fine powder suggested that amorphous material or solid dispersions of penciclovir within film components were not formed.

Table 1
Penciclovir concentration in polymer films pre- and post-casting

Cast film	Polymer film	
Penciclovir concentration (% (w/w))	Penciclovir concentration (% (w/w) ± S.D.; $n = 6$)	Relative standard deviation (%)
10.0	14.66 (0.32)	2.2
7.5	10.94 (0.26)	2.4
5.0	7.39 (0.17)	2.3
2.5	3.81 (0.12)	3.1
1.0	1.54 (0.05)	3.2
0.75	1.14 (0.03)	2.6
0.5	0.77 (0.03)	3.9
0.25	0.39 (0.015)	4.0
0.15	0.23 (0.003)	3.8
0.1	0.15 (0.004)	2.7
0.05	0.076 (0.002)	2.6
0.025	0.039 (0.001)	2.6

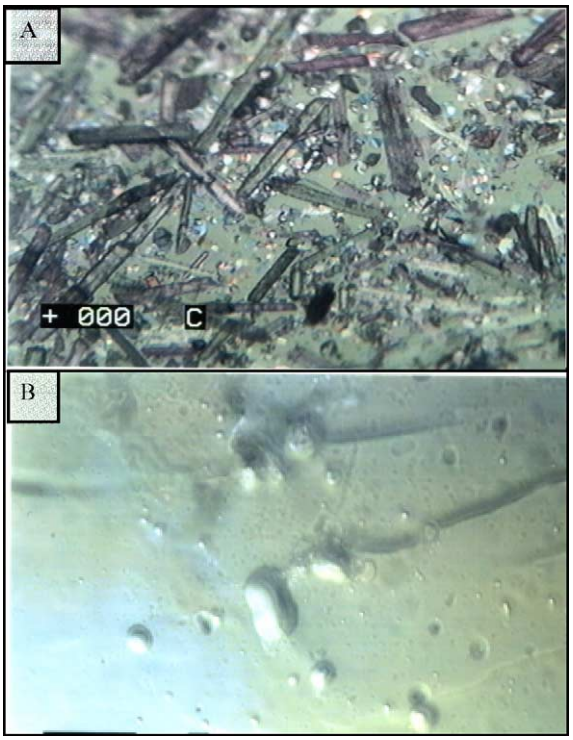

Fig. 1. Photomicrographs of penciclovir polymer film at (A) 14.66% (w/w) and (B) 1.5% (w/w) drug loading.

3.3. Differential scanning calorimetry

The penciclovir powder gave a single sharp endothermic peak with a melting point and enthalpy of fusion of 278 °C and 140 ± 5 J g^{-1} ($n = 3$) in agreement with product data sheet. Broad melting endotherms resulted at 276 °C for drug films (Fig. 2). As drug loading fell, the enthalpy of fusion correspondingly decreased up to 0.39% (w/w), beyond which no penciclovir melting events were recorded, implying that drug solubility was below 0.39% (w/w). The amorphous nature of the drug free films was shown by the absence of melting events and by a raised baseline;

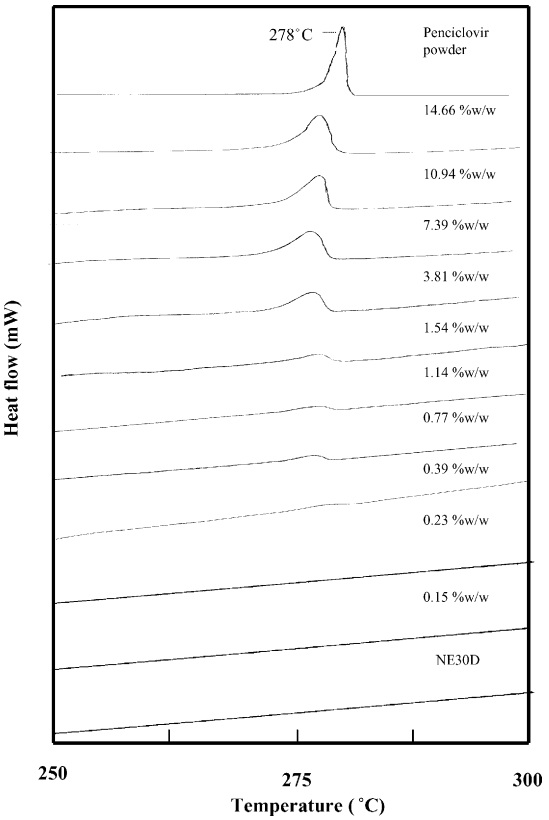

Fig. 2. Differential scanning calorimetry profiles (250–300 °C) of penciclovir powder, penciclovir-loaded polymer film at decreasing drug loading, and drug-free polymer film.

there were no interfering peaks at the drug melting point.

The theoretical enthalpy of fusion as a function of drug loading was calculated from that of pure drug:

$$\Delta H_t = x_p \, \Delta H_p \quad (2)$$

where ΔH_t and ΔH_p are the theoretical and pure penciclovir enthalpies of fusion, and x_p is the weight fraction of penciclovir [7]. Theoretical and experimental enthalpies were plotted versus drug loading (Fig. 3) resulting in linear calibration lines ($r^2 = 0.9989$ for experimental line); error bars on the theoretical lines were due to calculation from three values of ΔH_p. Experimental and theoretical lines agreed well. Since the theoretical line does not take into account the solubility of penciclovir in the film, whereas the experimental plot does, the difference between the two graphs

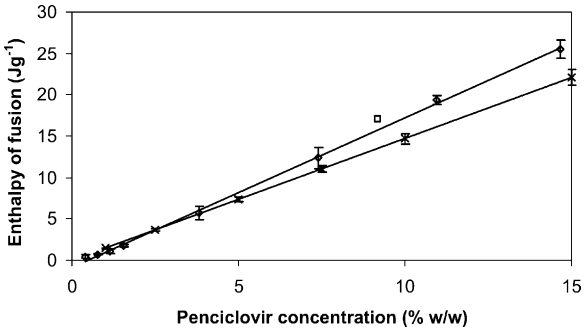

Fig. 3. (◇) Experimentally determined and (×) theoretically calculated enthalpy of fusion as a function of penciclovir loading in polymer films ($n = 3$). Error bars represent standard deviation.

could in principle be used to estimate drug solubility. However, in practice this approach was not possible since the experimental line overlapped that of the theoretical determination at low penciclovir levels and was raised above it at high drug levels. Higher than expected experimental enthalpies of fusion may have resulted because of drug interaction with the polymer; the broad endothermic event presented difficulties for an accurate determination of the integrated area. Additionally, the drug solubility was relatively low and, hence, the difference between theoretical and experimental lines was marginal; this approach may be more appropriate for systems with higher solubilities. Further difficulties arose due to the high water content in films (up to 25% (w/w)), the loss of which may further concentrate samples during analysis.

From the intercept of the experimental line a solubility of $0.44 \pm 0.12\%$ (w/w) ($n = 3$) was determined. This was close to <0.39% (w/w), which was the minimum drug concentration at which endotherms were observed on the thermograms. Thermal analysis results were higher than those estimated from visible microscopy (0.15–0.23% (w/w)) but used room temperature, whereas the DSC approach estimated solubility at the drug melting point. Thus, a higher value was expected for the thermal method.

For enthalpy of fusion values of penciclovir loaded films, precision of data expressed as %R.S.D. was good intra-batch (<5% R.S.D.) except for the 7.39 and 3.81% (w/w) samples where one outlying replicate caused a large %R.S.D. value for both intra- and inter-batch (Table 2). As expected, large R.S.D. values for inter-batch data resulted in comparison to

Table 2
Precision of differential scanning calorimetry data, intra- and inter-batches

Concentration of penciclovir in the polymer film (% (w/w))	Intra-batch		Inter-batch	
	Enthalpy of fusion (mean ± S.D., $n = 3$) ($J g^{-1}$)	Precision (%R.S.D.)	Enthalpy of fusion (mean ± S.D., $n = 3$) ($J g^{-1}$)	Precision (%R.S.D.)
14.66	25.9 (1.2)	4.6	24.3 (1.8)	7.4
10.94	19.4 (0.6)	3.4	19.8 (0.7)	3.5
7.39	13.2 (1.7)	13.0	10.9 (1.5)	13.7
3.81	6.1 (1.4)	23.0	4.8 (1.0)	20.8
1.54	1.9 (0.05)	3.0	1.6 (0.1)	6.2
1.14	0.9 (0.05)	5.0	1.3 (0.4)	30.0
0.77	0.8 (0.02)	3.0	0.6 (0.4)	66.0
0.39	0.7 (0.01)	2.0	0.24 (0.02)	8.3

intra-batch measurements. The use of <10 mg samples in analysis (drug content ranged from 0.025 to 10% (w/w)) especially as drug concentration reduced, increased the margin of error, indicating the heterogeneous nature of the samples. However, larger sample sizes (100 mg), such as those used to determine drug concentration in films, indicated homogeneity. A reduction in crystal size may improve the distribution of drug crystals and hence reduce errors experienced at small sample sizes.

Another problem inherent in this system was the large sample sizes utilized to improve sensitivity of the method, thus slower equilibration hence lag present between programmed and the actual temperature.

The calibration line was verified by preparing a film sample at 9.2% (w/w), where ΔH_t was 17.03 $J g^{-1}$. The difference between this sample and that predicted from the calibration line (16.2 $J g^{-1}$) was 5.4% similar to the %R.S.D. shown for inter-sample variability.

3.4. X-ray diffraction

The XRPD diffraction pattern of penciclovir (Fig. 4) agreed with literature; a single polymorphic form (needle crystals) was identified. The diffraction pattern of the drug-free film gave a raised baseline but no clear diffraction lines, characteristic for an amorphous material [15]. Therefore, peaks in the XRPD traces for drug-loaded films arose from penciclovir crystals. Qualitative analysis of the XRPD traces showed a decrease in the peak intensities as the weight fraction of penciclovir (x_p) fell. Peaks due to drug crystals were still present at an x_p value of 0.039 (0.39% (w/w)), but not at x_p of 0.023 (0.23% (w/w)). This indicated that the solubility of penciclovir in the films lies between these values or that the XRPD method was not sensitive enough to detect crystals below x_p of 0.039.

Theoretical predictions of intensity ratio ($I_{ip}/(I_{ip})_0$) as a function of weight fraction of penciclovir (x_p) were made [14,16–18]. The intensity (I) of line i of the penciclovir component ($_p$) in a film ($_f$) is given as:

$$I_{ip} = \frac{Kx_p}{\rho_p[x_p(\mu_p^* - \mu_f^*) + \mu_f^*]} \quad (3)$$

where K is a constant, ρ_p the density of penciclovir, x_p and μ_p^* are the weight fraction and mass attenuation coefficient (MAC) of penciclovir, and μ_f^* is the MAC of the film.

The intensity of peak i of a sample containing only penciclovir is given by:

$$(I_{ip})_0 = \frac{K}{\rho_p \mu_p^*} \quad (4)$$

Therefore, the ratio of intensities of line i in a penciclovir mixture to the identical line in a sample containing only penciclovir can be determined by dividing Eq. (3) by Eq. (4) to give the final intensity equation:

$$\frac{I_{ip}}{(I_{ip})_0} = \frac{x_p \mu_p^*}{x_p(\mu_p^* - \mu_f^*) + \mu_f^*} \quad (5)$$

The MAC of elements are available in the literature [19] and can be used to calculate the MAC value

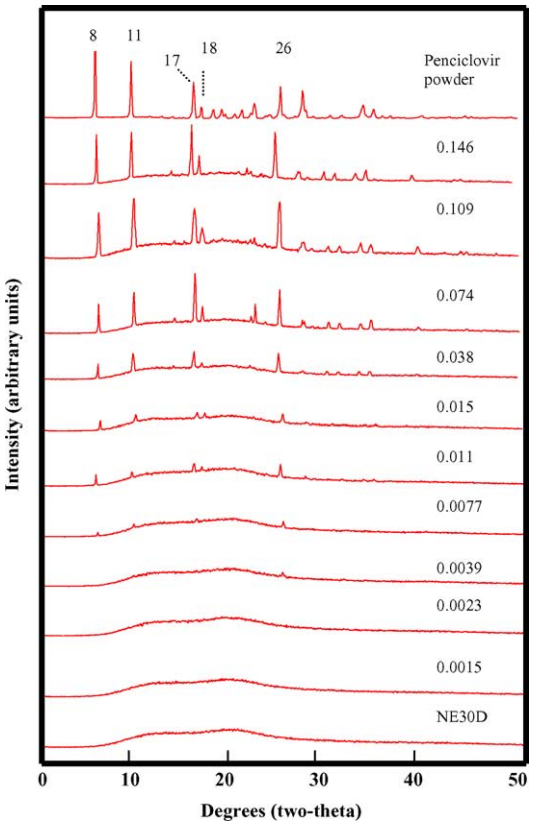

Fig. 4. X-ray powder diffractometry profiles (0–50° 2θ) of penciclovir powder, penciclovir loaded polymer film at decreasing weight fractions and drug free polymer film.

of a compound from its elemental composition using Eq. (6):

$$\mu^* = \sum_{k=1}^{n} w_k \mu_k^* \tag{6}$$

where w_k is the weight fraction of elements and μ_k^* are their respective MAC values. For penciclovir ($C_{10}N_5O_3H_{17}$), the weight fractions of elements (0.47, 0.27, 0.19, 0.07) and MAC of elements 4.6, 7.5, 11.5, 0.43, respectively [19], gave a calculated μ_p of 6.41 $cm^2\,g^{-1}$. The MAC of the film (μ_f) was the sum of the weight fraction of each compound in the film multiplied by the compounds MAC. Since the film consisted of poly-EA/MMA, PVP and water, the MAC was calculated for each compound first, resulting in values of 6.47, 5.50, 10.28 $cm^2\,g^{-1}$. In the film, the weight fraction of the film components

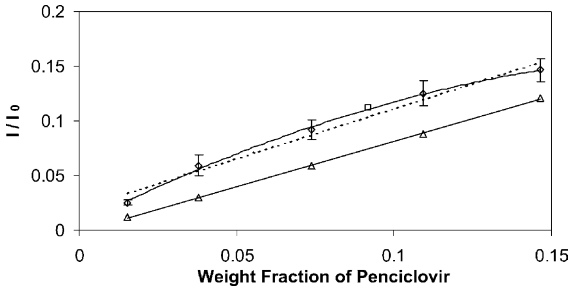

Fig. 5. (◇) Experimentally determined and (△) theoretically calculated mean intensity ratio as a function of weight fraction of penciclovir in polymer films ($n = 3$). Error bars represent standard deviation. (Linear regression analysis and polynomial fit of the experimental data was performed.)

depended on the drug content. At the highest weight fraction (penciclovir:film ratio of 0.15:0.85 of which 0.45 was poly-EA/MMA, 0.1 PVP and 0.45 water) the μ_f^* was calculated to be 7.98 $cm^2\,g^{-1}$. At the lowest penciclovir weight fraction (ratio of 0.01:0.99 penciclovir:film) the μ_f^* determined was 8.24 $cm^2\,g^{-1}$. Therefore, the MAC used was calculated for an intermediate composition, 0.08:0.92 penciclovir:film, a value of 8.11 $cm^2\,g^{-1}$ resulted and was used in all the calculations.

The determination of μ_f^* and μ_p^* allowed theoretical determination of intensity ratio as a function of x_p, a plot of which (Fig. 5) was found to be linear ($r^2 = 0.999$). In simple powder mixes, for example, β-and δ-mannitol [20], or mixtures of crystalline and amorphous leukotriene biosynthesis inhibitor (MK-0591) [15], the MAC of the unknown and film components were the same. In a multicomponent system like ours with different MAC values for unknown and film, although a linear relationship, resulted the slope was not 1 but of 0.83. In some cases a linear relationship does not result and the data has to be fitted to a modified form of Eq. (5) [17].

To determine the $(I_{ip})_0$ from the pure penciclovir trace and I_{ip} as a function of x_p, integrated intensities of five of the most intense peaks were summed for each trace. More than one peak was utilised to minimize the influence of preferred orientation on peak intensity. Peak area instead of peak height was selected since variations in particle size range affect peak shape and hence height, but does not influence peak area [18]. The $I_{ip}/(I_{ip})_0$ ratio as a function of x_p was calculated from the experimental data, and a plot was non-linear;

regression analysis gave r^2-value of 0.979 with a slope of 0.91 (Fig. 5).

The theoretical and experimental intensity ratio plots agreed poorly, due to the dynamic and complex nature of the multicomponent system with different MAC values (Fig. 5). The film results depended on the ratio of components, which had been estimated from the weight of the dry film. Since the polymer film contained a high weight fraction of water (0.40–0.45), fluctuations in its content would affect the experimentally determined values and hence differ from the theoretical. Other sources of error included the fraction of drug dissolved in the film and possible formation of amorphous solid dispersions, with drug precipitating out on drying of cast films. Suryanarayanan et al. [14] associated the large variance in the estimation of integrated peak intensity to amorphous scattering of X-rays by the non-crystalline ingredients. The difference in the theoretical and experimental line could possibly be exploited to give a solubility value. However, the experimental line was above theoretical and, since large errors were associated with it, the assessment was not possible. Use of this difference could potentially be of value in a system were the drug had a high solubility.

The calibration curve was verified by preparing an additional film at 9.2% (w/w), which provided an intensity ratio of 0.112; the difference between this value and that from the calibration plot 0.105 was 6.7%.

The precision of the X-ray data expressed as %R.S.D. was again lower intra-batch than inter-batch (see Table 3). The maximum R.S.D. of 3.8% intra-batch gave an indication of the instrumental errors, whereas the inter-batch maximum value of 16.2% R.S.D. resulted from a combination of instrumental errors and between-batch sample preparation differences.

Solubility calculated from the x intercept of the intensity ratio versus x_p gave $-1.68 \pm 0.43\%$ (w/w) from linear analysis, thus the relationship is non-linear. A curve-fit of the experimental data gave a correlation coefficient of 0.9976, with an intercept $x_p = 0.053$ (0.53% (w/w); Fig. 5). Suryanarayanan et al. [14] successfully estimated the solubility of salicylic acid in a hydrogel at 20% (w/w) using XRPD. In our system, the solubility was <0.5% (w/w). Due to the relatively large instrumental and experimental errors associated with the method, it was deemed unsuitable for solubility determinations at very low concentrations.

Numerous sources of error have been identified in quantitative XRPD analysis (e.g. [14,17]). Hurst et al. [21] separated errors associated with the XRPD method into three groups; instrumental, inherent properties of the compound and parameters related to preparation and mounting of samples. Some of these errors may have had a significant impact in our X-ray analysis.

Preferred orientation is the non-random crystal packing in X-ray holders and is especially problematic with powder mixtures; it can give an error in peak intensity of up to 100%. Grinding samples and filling holders from the side usually combat this. In our system, this effect was minimised since the drug crystals were randomly oriented in a viscous semi-solid vehicle. Upon casting the film and drying, the crystals remained randomly oriented throughout the matrix (see Fig. 1). This was reflected in the diffraction pattern, where reproducible intensities resulted (Fig. 4).

Another possible error arises from microabsorption effects [16]. When two substances of different MAC

Table 3
Precision of X-ray powder diffractometry data, intra- and inter-batches

Concentration of penciclovir in the polymer film (% (w/w))	Intra-batch		Inter-batch	
	Sum of integrated intensities (mean ± S.D., $n = 3$; AU × 2θ)	Precision (%R.S.D.)	Sum of integrated intensities (mean ± S.D., $n = 3$; AU × 2θ)	Precision (%R.S.D.)
14.66	2530 (43)	1.7	2434 (168)	7.0
10.94	2109 (32)	1.5	2082 (189)	9.1
7.39	1479 (32)	2.1	1527 (156)	10.3
3.81	1044 (40)	3.8	987 (160)	16.2
1.54	440 (13)	3.0	421 (40)	9.3

mix, this affects the accuracy of the intensity measurements. Since MAC of penciclovir (6.41 $cm^2\,g^{-1}$) and the film (8.11 $cm^2\,g^{-1}$) are different, errors due to microabsorption need to be considered.

Sample thickness also requires consideration and should be adequate to prevent loss in intensity. The required sample thickness can be estimated from [17]:

$$l \geq \frac{3.2 \sin\theta}{\mu^* \rho'} \tag{7}$$

where l is the sample thickness, θ the incident angle of the X-rays (8–26°), μ^* the mass attenuation coefficient of the sample and ρ' the density. The density was calculated from sample area (7.1 cm^2), thickness (0.05 cm ± 0.01 cm) and weight (0.2 ± 0.03 g), the density value was 0.63 $g\,cm^{-3}$. The value of μ^* ranged from 7.8 $cm^2\,g^{-1}$ (x_p, x_f = 0.15, 0.85) to 8.3 $cm^2\,g^{-1}$ (x_p, x_f = 0.01, 0.99). Therefore, an intermediate value of 8.1 $cm^2\,g^{-1}$ was used in the calculation. The l value resulting for 2θ values of 8° is $l > 0.08$ and for 26° was $l > 0.27$ cm. Since the average sample thickness (0.05 cm) was less than that calculated for maximum diffracted intensity, results may have been erroneous through intensity loss due to inadequate sample thickness.

3.5. Release kinetics

Higuchi [2,22] stated that release from a planar system having dispersed drug (suspension) or dissolved drug (solution) in a homogeneous film should follow the relationship:

$$\text{suspension} \quad Q = [D(2A - C_S)C_S t]^{1/2} \tag{8}$$

$$\text{solution} \quad Q = 2A\left(\frac{Dt}{\pi}\right)^{1/2} \tag{9}$$

where Q is the amount of drug released after time t per unit exposed area, D the diffusivity of the drug in the film, A the initial total drug concentration, and C_S the drug solubility in the matrix.

Both equations describe drug release as being linear with the square root of time:

$$Q = k_H t^{1/2} \tag{10}$$

For a homogeneous suspension:

$$k_H = [D(2A - C_S)C_S]^{1/2} \tag{11}$$

and for a homogeneous solution:

$$k_H = 2A\left(\frac{D}{\pi}\right)^{1/2} \tag{12}$$

where k_H is the release rate constant, the slope of a plot Q versus $t^{1/2}$.

Several assumptions apply for Eqs. (8) and (9) including that the drug is homogeneously distributed throughout the vehicle, that only the drug diffuses out and that sink conditions prevail. Providing these conditions are met, then a plot of Q versus $t^{1/2}$ should be linear for at least 30% of loaded drug released [2] as verified by Bodomeier and Paeratakul [8,23].

Drug release from the films followed Higuchi kinetics so a plot of cumulative amount released versus square root of time was linear. An initial 'burst' release preceded a constant release rate phase (Fig. 6A). The initial rapid release can be attributed to dissolved drug and crystals at the film surface [8,23]. The second phase had a lower release rate than the first due to the receding boundary layer; drug must dissolve prior to diffusion through the film for suspensions, thus reducing release rate.

The release rate constant obtained from the slope of Higuchi plots increased as drug concentration in the films rise. This elevation in release rate constant was greater (0.0041 mcg $cm^{-2}\,min^{-1/2}$) when drug was dissolved because the concentration gradient between film and sink increased as drug loading approached saturation. Beyond saturation, when excess drug was suspended, the increase in the release rate constant as a function of drug loading was at a slower rate (0.0005 mcg $cm^{-2}\,min^{-1/2}$) since the concentration gradient was at its maximum and drug has to dissolute to maintain the concentration gradient. Hence, a plot of rate constant for each film as a function of drug loading revealed two slopes. Linear regression analysis of data when drug was dissolved in the film gave a straight line, r^2 = 0.999 and slope = 0.0041 mcg $cm^{-2}\,min^{-1/2}$. When drug was in excess (suspension), gave a straight line, r^2 = 0.999 with a slope = 0.0005 mcg $cm^{-2}\,min^{-1/2}$. Extrapolation of both lines (dotted lines in Fig. 6) to intersection estimated drug solubility. The solubility of penciclovir in the polymer film determined from this method was 0.42% (w/w), close to that estimated from visible microscopy studies.

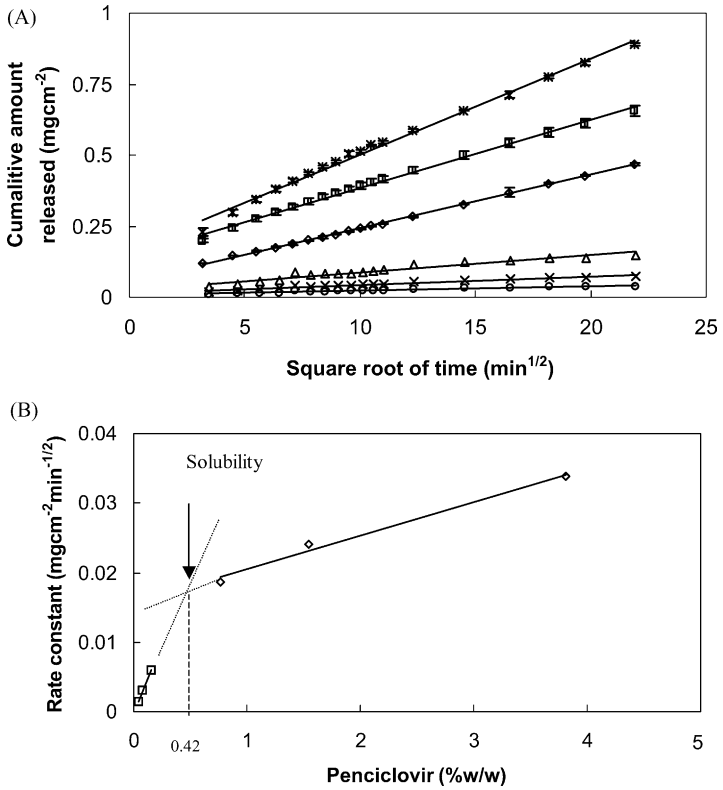

Fig. 6. (A) Higuchi square root of time plots for penciclovir release from polymer films. ((○) 0.039, (△) 0.076, (◇) 0.15, (×) 0.77, (□) 1.54, (✱) 3.81% (w/w)). (B) Release rate constant determined from Higuchi plots as a function of drug loading. ((□) drug dissolved in the film, (◇) drug dissolved and suspended in the film, (. . .) extrapolation of best fit lines).

3.6. Comparison of techniques

A summary of the advantages and disadvantages of these solubility techniques is shown in Table 4. The visible microscopy (VM) method was simple, rapid and, together with the XRPD technique, was non-destructive and, thus, could be conducted prior to DSC and drug release studies, where samples were destroyed. Besides VM, the other approaches were more complex, time consuming, data analysis was complex and expensive instrumentation was required. VM detected crystal fragments to the lowest level (0.23% (w/w)), i.e. was most sensitive, whereas XRPD and DSC detectable levels from visual observation of thermograms and diffractograms was 0.39% (w/w). The sample size in DSC was <10 mg, whereas for XRPD this was 200 mg; thus for the sample size used the DSC was more sensitive then the XRPD method. Data collected from VM was qualitative; XRPD and DSC data were qualitative and quantitative but with release studies only quantitative data could be collected.

The VM procedure allowed observation of crystal size range, shape and distribution. The active did not have to be crystalline since amorphous powders could possibly also be observed, as was the case for release studies. For DSC and XRPD the drug had to be crystalline. Additional data besides solubility determination from DSC was drug melting point and enthalpy of fusion; changes to these from the pure drug could indicate impurities, drug vehicle interactions and polymorphic transitions. With the XRPD, different polymorphs could be identified and crystalline samples may be distinguished from amorphous material. The release studies allowed the release kinetics of the formulation to be determined.

Table 4
Summary of the main advantages and disadvantages of the techniques used in solublility studies

	Advantages	Disadvantages
Visible microscopy	• Quick, simple, non-destructive • Highly sensitive • Can observe crystal shape, size distribution and homogeneity • Gives a good estimate of drug solubility • Active does not have to be crystalline	• Data is qualitative
DSC	• Observe changes in drug melting point, impurity or polymorphs melting transitions • Small samples required <l0 mg • Qualitative data gives idea of solubility range • Quantitaive data gives good idea of solubility value • Linear calibration plots can be constructed	• Time consuming, complex, destructive • Active has to be crystalline • Estimate of solubility is at drug melting point • Moderate sensitive
XRPD	• Non-destructive • Quantitative data gives idea of solubility range • Linear calibration plots can be constructed • Useful in identifying compound and polymorphs • Amorphous compounds do not interfere	• Time consuming, complex • Moderate sensitivity • Quantitative data gives poor idea of solubility value • Data analysis is complex, large sources of error • Active must be crystalline • Large sample size required (0.2 g)
Release data	• Active can be crystalline or amorphous • Gives good estimate of solubility • Data is quantitative • Gives release kinetics of the formulation	• Time consuming, complex, destructive • Sample size of 0.2 g required

The observed VM, DSC and XRPD data gave a consistent range for the solubility of penciclovir in polymer films. A value of 0.15–0.23% (w/w) was determined for VM and <0.39% (w/w) for DSC and XRPD traces. Quantitative analysis gave values of 0.44% (w/w) for DSC, 0.53% (w/w) from XRPD data and 0.42% (w/w) from release studies. From these results, the solubility value expected should be within the range identified by VM studies and the values resulting from other techniques were close to this range.

Theoretical and experimental calibration lines were different. Hence, theoretical predictions cannot be relied upon, the data should be experimentally deduced for systems in which drug solubility is low.

4. Conclusions

Few analytical techniques can determine accurately the physical state (solution/suspension) and solubility of drugs in a semi-solid or polymer film. The simplest approach that detected solid drug at the lowest levels was visible microscopy. Other techniques had merits, differential scanning calorimetry (DSC) and X-ray powder diffractometry (XRPD) were useful to characterise drug as well as determine solubility; release data could be used to deduce release kinetics and diffusion coefficient. Solubility values of penciclovir in Eudragit NE30D films were between 0.15 and 0.23% (w/w) for visible microscopy, 0.44% (w/w) from DSC, 0.53% (w/w) from XRPD and 0.42% (w/w) from release studies.

Acknowledgements

The author would like to thank EPSRC and SKB for providing financial support for this project.

References

[1] A.C. Williams, Transdermal and Topical Drug Delivery: From Theory to Clinical Practice, Pharmaceutical Press, London, 2003.
[2] T. Higuchi, J. Soc. Cosmet. Chem. 11 (1960) 85–97.

[3] B. Narasimhan, in: D.L. Wise (Ed.), Handbook of Pharmaceutical Controlled Release Technology, Marcel Dekker, New York, 2000, pp. 155–183.
[4] G.R. Todd, Pharmaceutical Codex, Pharmaceutical Press, London, 1979.
[5] N. Kobayashi, I. Saitoh, Chem. Pharm. Bull. 46 (1998) 1833–1835.
[6] A. Gopferich, G. Lee, Drug Dev. Ind. Pharm. 18 (1992) 319–331.
[7] F. Theeuwes, W. Higuchi, J. Pharm. Sci. 63 (1974) 427–429.
[8] R. Bodomeier, O. Paeratakul, Pharm. Res. 6 (1989) 725–730.
[9] M. Jenquin, J. McGinity, Int. J. Pharmcol. 101 (1994) 23–34.
[10] A.S. Cantor, J. Contr. Rel. 61 (1999) 219–231.
[11] S.M. Wick, A.S. Cantor, Determination of Drug Solubility Within Drug-in-Adhesive Systems. Perspectives in Percutaneous Penetration, Cardiff, UK, 2000.
[12] L. Chafetz, D.C. Tsilifonis, C. Moran, J. Pharm. Sci. 63 (1974) 1771–1773.
[13] Z.T. Chowhan, R. Pritchard, J. Pharm. Sci. 64 (1975) 754–759.
[14] R. Suryanarayanan, S. Venkatesh, L. Hodgin, P. Hanson, Int. J. Pharmcol. 78 (1992) 77–83.
[15] S. Clas, R. Faizer, R. O'Connor, E. Vadas, Int. J. Pharmcol. 121 (1995) 73–79.
[16] H.P. Klug, L. Alexander, X-ray Diffraction Procedures for Polycrystalline and Amorphous Materials, Wiley, New York, 1974.
[17] R. Suryanarayanan, C. Herman, Int. J. Pharmcol. 77 (1991) 287–295.
[18] R. Suryanarayanan, in: H.G. Brittan (Ed.), Physical Characterization of Pharmaceutical Solids, Marcel Dekker, New York, 1995, pp. 187–222.
[19] C.H. Macgillavry, G.D. Rieck, International Tables for X-ray Crystallography, Reidel, Holland, 1983.
[20] S.N. Campbell Roberts, A.C. Williams, I.M. Grimsey, S.W. Booth, J. Pharm. Biomed. Anal. 28 (2002) 1149–1159.
[21] V.J. Hurst, P.A. Schroeder, R.W. Styron, Anal. Chim. Acta 337 (1997) 233–252.
[22] T. Higuchi, J. Pharm. Sci. 50 (1961) 874–875.
[23] R. Bodomeier, O. Paeratakul, Int. J. Pharmcol. 59 (1990) 197–204.